

Laboratory tests and numerical studies of a geosynthetic reinforced pile-supported embankment

Yining Hu^{1*}, Laurent Briançon¹, and Daniel Dias²

¹ INSA LYON, GEOMAS, 69621 Villeurbanne, France

² Université Grenoble Alpes, CNRS, Grenoble INP, 3SR, 38000 Grenoble, France

Abstract. This paper presents laboratory tests examining geosynthetic-reinforced pile supported-embankments over soft soil. Many tests were carried out in a 4m x 4m x 0.9m pit including 16 piles, varying the load transfer platform thickness and geosynthetic reinforcement. A comprehensive monitoring program was implemented to track the load transfer inside the granular platform and the settlement. This research is a part of the cooperative national research project ASIRI+ (2019 - 2024) which gathers about forty organizations and aims to propose dimensioning rules in the field of soil reinforcement by rigid inclusions. These experimental results investigated the understanding of complex mechanisms developed inside the load transfer platform to evaluate the efficiency of the geosynthetic. In addition, a numerical model established by the software FLAC3D was employed to simulate the experimental tests. The ability of the numerical model to account for the settlement of the granular soil surface and the stress transmitted to the top of the subgrade layer was established by comparisons with the experimental data. From this calibrated numerical model, many simulations were performed to propose an optimal solution for the reinforcement by the geosynthetic.

1 Introduction

Over the past few decades, rapid urbanization and infrastructure development have increasingly required construction on weak, highly compressible soils. To address this challenge, pile-supported embankments (PSE) have emerged as a widely adopted soil reinforcement technique since the 1990s. This system combines rigid inclusion piles installed in soft soils with a Load Transfer Platform (LTP) that effectively distributes loads to the pile heads. The LTP typically consists of granular materials like sand or gravel.

To improve the efficiency of this composite foundation, one or several layers of geosynthetics can be inserted within the granular mattress. These horizontal reinforcements improve the load transfer to the piles through the membrane effect.

Additionally, for evaluating the limit state requirements or studying the behavior of a geosynthetic reinforced pile-supported embankment (GRPSE), experimental investigations,

* Corresponding author: yining.hu@insa-lyon.fr

numerical modelling techniques are commonly used in the literature. The experimental approach comprises full-field tests or scaled model tests. Le Hello and Villard [1] presented a series of four full-scale instrumented experiments, and the membrane effect of geosynthetics was observed. The load, which is not transferred by arching effect, is transmitted to the geotextile which is deforming in membrane. The geosynthetic sheet's displacement depends on the load applied and the stiffness of the geosynthetics sheet used. The efficiency of the geosynthetics had also been highlighted in the frame of the first French project ASIRI [2]. Eekelen et al. [3] presented a series of nineteen 3D model experiments on piled embankments, and have found that the calculated Geogrid (GGR) strains using current analytical models exceed the GGR strains measured in the field and proposed a new design method inserted in the Dutch Standard CUR226 [4]

The numerical modelling provides a helpful and powerful tool to understand the complicated behavior of GRPSE. In this approach, the finite element method, finite difference method, and discrete element method are commonly used. Being as important as the design methods, these analysis approaches are an essential part of any geotechnical design. The three aforementioned approaches can be used separately or in combination with one another. The choice of the most relevant approach(es) depends on the needs of the designers in different application scenarios.

While many experimental and numerical studies have investigated GRPSE systems [5-11], current design standards and recommendations provide guidance for LTP design, questions remain about the choice between geotextiles and geogrids, the optimal geosynthetic configuration, including number, type, and positioning within the mattress. Even if the geosynthetic reinforcement seems to improve the load transfer to the piles, its role on the settlement reduction or its part in the load transfer remain not well understood.

As part of the French national project ASIRI+ (2019-2025), which is the extension of ASIRI project (2005-2012), researchers are testing various LTP configurations to better understand their mechanisms and efficiency. A particular challenge in laboratory testing of PSE is identifying an analog material that can reliably simulate soft soil compressibility while ensuring the reproducibility of the tests.

In the present research, a laboratory test at a scale $\frac{1}{2}$ was conducted using an experimental bench containing 16 rigid inclusions. The test setup consisted of three layers: a 60 cm layer of rubber granulates (Deltagom) simulating soft soil, a 25 cm layer of gravel, and a 50 cm layer of sand. 3D numerical analyses are carried out using a finite difference method, incorporated in the Fast Lagrangian analysis of continua FLAC3D [12].

2 Experimental Study

2.1 Test Facilities

Laboratory tests were conducted in a 4m x 4m x 0.9m experimental pit to investigate load transfer mechanisms within pile-supported embankments. The pit contained 16 rigid inclusions, each with a 15cm diameter, arranged as illustrated in **Fig.1**. It should be noted that only the central area of the pit, encompassing the four inclusions of the central mesh, is instrumented in order to avoid boundary effects due to the pit walls.

The embankment consisted of three distinct layers. The bottom layer comprised 60cm of rubber granulates (Deltagom) surrounding the rigid piles. Rubber granulates were selected for their large deformation characteristics, which simulate soft soil behavior without requiring consolidation time. Above this, a 25cm gravel layer was installed, followed by a 50cm sand layer at the top. The fill stage is shown in **Table 1**.

Table 1. Fill stages and model building steps

Fill stages	Model building steps
1	Installation of rubber granulates (Deltagom) layer with rigid inclusions (RIs), followed by displacement field initialization
2	Placement of gravel layer (load transfer platform), followed by displacement field initialization
3	Completion of sand layer placement

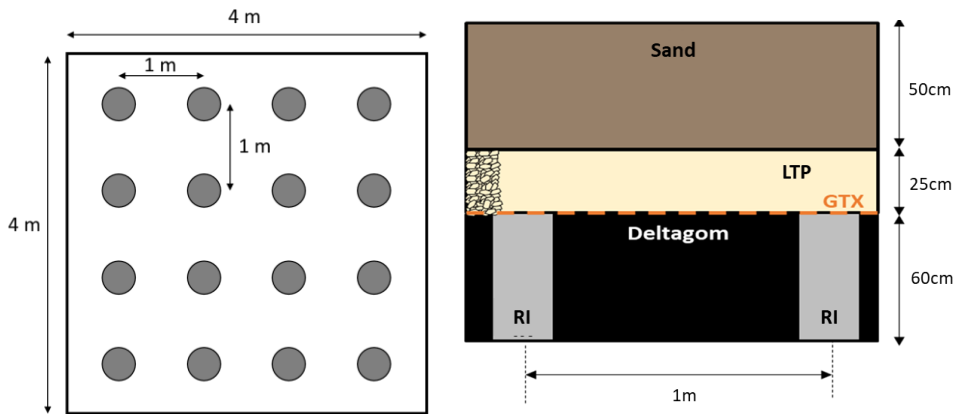


Fig. 1. The schematic figure of the laboratory test configuration.

The first test, carried out without horizontal reinforcement, served as the reference test for the dimensioning of the geosynthetics. Note that each material layer is separated by a nonwoven geotextile (not designed for reinforcement) to prevent cross-contamination, as materials are reused between tests.

With regards to the second test, the crossed monoaxial geotextiles were installed directly on the head of the rigid inclusions. The parameters of the geosynthetics used are presented in **Table 2**.

Table 2. The strength parameter of geotextile

Parameter	Specification	Standard
$J_{(SP)}$	3000-3500 kN/m at $\epsilon = 2\%$	NF EN ISO 10319
$J_{(ST)}$	Negligible at $\epsilon = 2\%$	NF EN ISO 10319

* $J_{(SP)}$ is the stiffness in principal direction, $J_{(ST)}$ is stiffness in transverse direction and ε is represents strain - the percentage of elongation experienced by the material when subjected to tensile forces.



Fig. 2. The configuration of the laboratory tests and installation of the geotextile.

2.2 Instrumentation

Earth Pressures Cells (EPC) were installed on the pile head and on the soil at various elevations to measure the load transfer (**Fig. 3**). Settlement Sensors (SS) were installed in the soil, at strategic positions, in order to follow the settlement of the soft soil, the deformation of the LTP, and locate the plane of equal settlement in the backfill. The central grid was particularly monitored (**Fig. 3**). These sensors measure displacement through hydraulic pressure variations. Transmitters at the same level are connected in series to a reservoir mounted on a fixed support outside the test bench. The water reservoir maintains saturated sensor circuits at constant water pressure. The transmitter measures pressure difference between its position and the reservoir.

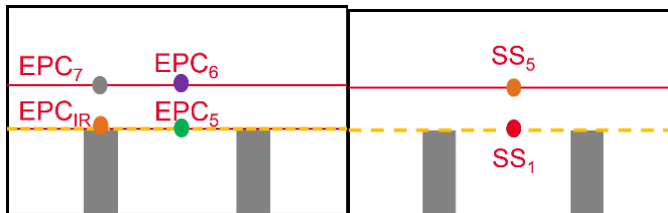


Fig. 3. Location of EPC and SS

Data was recorded using a Data Logger which can be programmed remotely. Each sensor connects to a pre-configured channel, with customizable measurement intervals. While data is stored in the system's internal memory, it can be exported to a computer. This logger was used to record static settlement values from hydraulic settlement sensors and static vertical pressures.

3 Experimental Results

The test results reveal significant differences between reinforced and unreinforced conditions across multiple loading stages.

The incorporation of a geotextile shows no substantial influence on the characteristic patterns of the stress evolution. Nevertheless, a systematic comparison of the results remains necessary.

The first test, carried out without horizontal reinforcement, was considered the reference test for the design of the geosynthetics. After adding gravel on the rubber granulates layer, stresses of 4 kPa (EPC_5) and 18 kPa (EPC_{IR}) were recorded, resulting in a 3 cm settlement (SS_5). These values are aligned with theoretical calculations based on the material weight and height.

Following the addition of 50 cm sand, stress measurements revealed varying pressures across measurement points, with EPC_5 at 4 kPa, EPC_6 at 7 kPa, EPC_7 at 25 kPa, and EPC_{IR} at 180 kPa, generating settlements of 3.8 cm (SS_1) and 3 cm (SS_5). The significant stress increase on the inclusions indicated soil arching formation and demonstrated the load transfer to the rigid inclusions.

In comparison to the unreinforced case, the geotextile-reinforced system demonstrated enhanced performance. The settlement at SS_1 significantly decreased to 1.1 cm, while stresses increased markedly across measurement points: EPC_5 rose to 7 kPa, EPC_7 to 30 kPa, and EPC_{IR} to 232 kPa. The membrane effect of the geotextile reinforcement improved the load transfer mechanism, directing more stress onto the rigid inclusions and resulting in more efficient soil arching development and better settlement control.

4 Numerical Analysis

The finite difference software FLAC (Fast Lagrangian Analysis of Continua) 3D, developed by Itasca Consulting Group, Inc., was adopted for this numerical analysis. **Fig. 4** shows the overview of the numerical model for this case study.

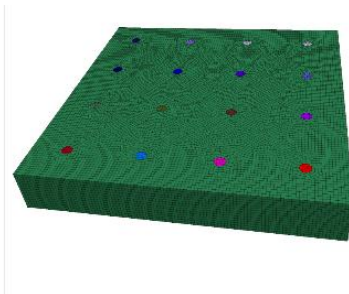


Fig. 4. Overview of the numerical model

No deformations are assumed below the substratum. The bottom boundary is fixed in all three directions and the four vertical sides are blocked in their normal direction. The unit cell in this study is modeled using 20,305 zones for the soils. The initial parameters used in the numerical analysis are presented in **Table 3**. For the geotextile material, it demonstrated a stiffness of 3.5×10^6 N/m.

In the numerical modeling, different constitutive models were employed. The gravel was modeled as a linear elastic perfectly plastic material with the Mohr-Coulomb failure criterion, while the soft soil and rigid inclusions behavior was simulated using a linear elastic model.

The numerical model followed three calculation steps. Firstly, the soft soils and rigid inclusions are installed, then an equilibrium under self-weight is reached. In the next step, a LTP layer of 25cm thickness is placed on the pile top. One geosynthetic layer is installed in the middle of the LTP and the pile head top. Finally, the embankment is set up to 0.5 m. An illustration of the model is shown in **Fig.1**. Based on the initial strength parameter, the numerical results are illustrated in **Fig. 5**.

Table 3. Input parameters for the numerical simulations

Material	Young modulus kN/m ²	Poisson ratio	Weight kN/m ³	Cohesion kN/m ²	Friction angle (°)
Rubber granulates	84	0.25	10	/	/
Gravel	50x10 ³	0.3	17	5	35
Rigid inclusion	11.5x10 ⁶	0.2	24	/	/
Sand	35x10 ³	0.3	19.68	10	38

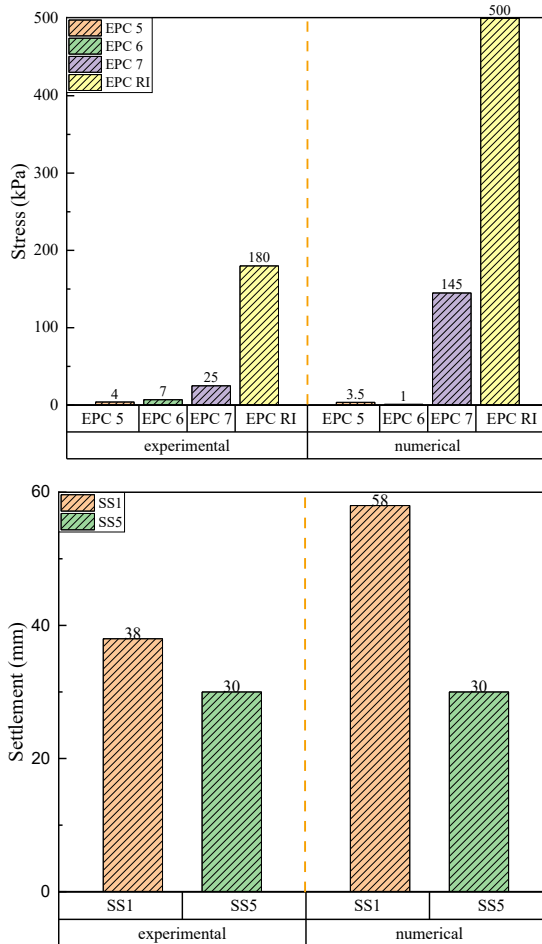


Fig. 5. Comparison of the vertical stress and vertical displacement between experiment and numerical simulation (initial simulation)

The comparison between numerical and experimental results revealed notable discrepancies, particularly in the rigid inclusion head stress, where the numerical simulation significantly overestimated the values observed in the experimental tests.

Despite multiple attempts to calibrate the strength parameters of various materials, the rigid inclusion head stress showed a minimal variation. This persistent discrepancy can be

attributed to the significant stiffness contrast between the rigid inclusion and soft soil, suggesting the crucial role of the interface behavior. Subsequently, the incorporation of interface elements into the model yielded substantially improved agreement with experimental results, and other parameters used in numerical simulation are presented in **Table 4**.

Table 4. Adapted parameters for numerical simulation after calibration

Material	Young modulus kN/m ²	Poisson ratio	Weight kN/m ³	Cohesion kN/m ²	Friction angle (°)
rubber granulates	Illustrated in Fig.5	Illustrated in Fig.5	10	/	/
Gravel	50x10 ³	0.3	17	5	37
Rigid inclusion	11.5x10 ⁶	0.2	24	/	/
sand	35x10 ³	0.3	19.68	10	38
Interface (between rigid inclusion and soft soil)	$K_n=2 \times 10^{10}$, $K_s=2 \times 10^{10}$ (kN/m ³)				

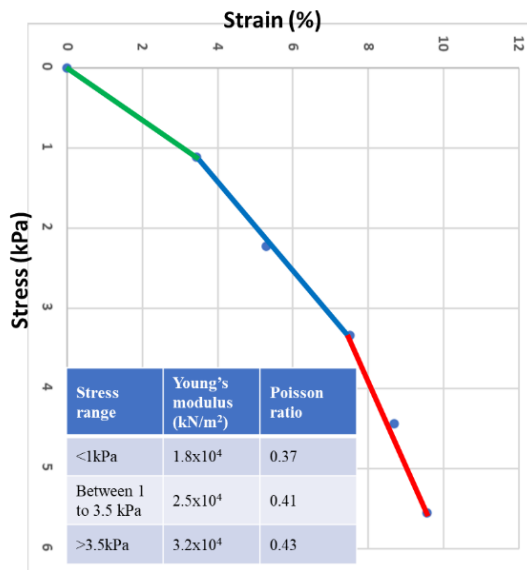


Fig. 6. Stress-strain behavior and properties of rubber granulates under different loading phases

Oedometer tests demonstrated that the rubber granulates exhibit stress-dependent hardening behavior. To characterize this behavior, we calibrated a unit cell model in FLAC3D to determine the material parameters. The calibration results, as shown in the figure, indicated that the Young's modulus ranges from 1.8×10^4 to 3.2×10^4 kN/m², with Poisson's ratio varying between 0.37 and 0.43.

Similarly, the numerical simulation was conducted in three distinct stages (Stage 1, Stage 2, and Stage 3), representing the sequential construction process of the embankment. Each stage corresponds to the progressive addition of fill layers, thereby simulating the actual construction sequence. The vertical stress profile shown in **Fig. 7** demonstrates a general pattern with negative values indicating compression. The EPC_{IR} value is specifically

measured at the 1.5 m position, corresponding to the first stress concentration zone. The numerical results are presented in **Fig. 8**.

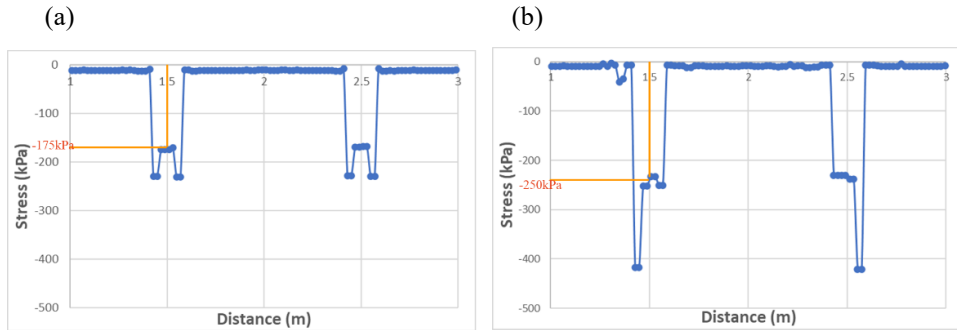


Fig. 7. Numerical analysis of the multi-stage embankment construction (a) profile of vertical stress without reinforcement (b) profile of vertical stress with reinforcement

Comparison between measured data and numerical analyses showed a strong agreement (**Fig. 8**). Furthermore, the difference of rigid inclusion head stress is 5.5%, which is acceptable and a reasonably good agreement can be concluded between the numerical model and experimental data. Therefore, the comparison results proved that this numerical model is reasonable and reliable for the analysis of GRPSE. After inserting the geotextile, the load transfer efficiency is 43%.

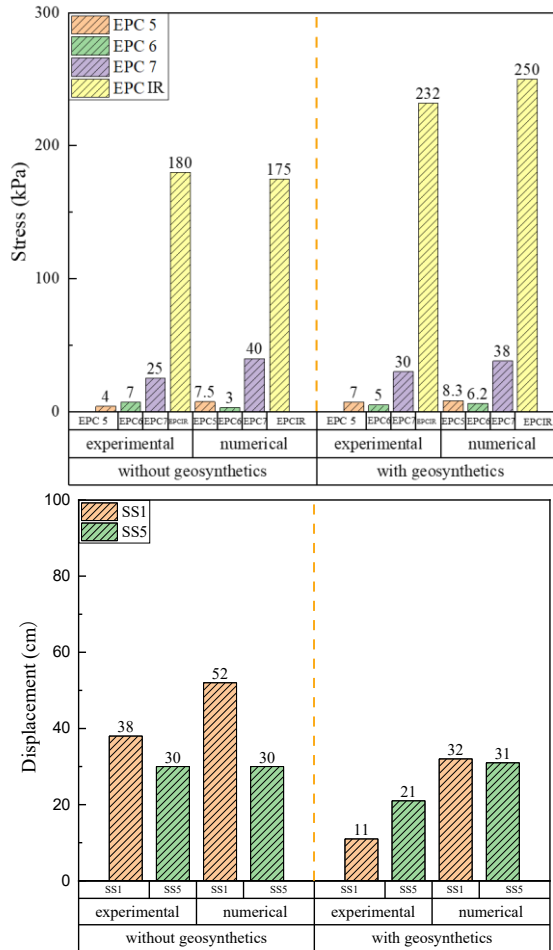


Fig. 8. Comparison of the vertical stress and vertical displacement between experiment and numerical simulation

5 Conclusion

Laboratory tests were conducted on a pile-supported embankment to investigate the settlement and load transfer occurring during an embankment installation. The experimental results demonstrated a significant enhancement in load transfer mechanisms with the incorporation of a geotextile reinforcement. When compared to the unreinforced system, the reinforced configuration exhibited a notable increase in stress concentration on the rigid inclusions (up to 232 kPa), while surface settlement was reduced by over 70% (from 3.8 cm to 1.1 cm). The efficiency is improved by the presence of the geosynthetic.

These experimental results were effectively validated through numerical modeling, which accurately predicted both surface settlements and stress distributions. However, the model requires a calibration, incorporating interface elements and the non-linear mechanical behavior of rubber granulates, to successfully reproduce the experimental observations. This validated numerical model serves as a valuable tool for optimization studies, supporting the development of design guidelines for geosynthetic reinforcement in similar ground improvement scenarios. This integrated experimental-numerical approach provides a robust

framework for understanding and designing geotextile-reinforced soil systems supported by rigid inclusions.

Acknowledgements This work was carried out as part of the national ASIRI+ project. The authors would like to thank all the members of this project for their support.

References

1. B. Le Hello, P. Villard, Embankments reinforced by piles and geosynthetics— Numerical and experimental studies dealing with the transfer of load on the soil embankment, *Eng. Geol.* **106**, 1, 78–91 (2009). doi: 10.1016/j.enggeo.2009.03.001.
2. L. Briançon, B. Simon, Performance of pile-supported embankment over soft soil: Full-scale experiment, *J. Geotech. Geoenvironmental Eng.* **138**, 4, 551–561 (2012). doi: 10.1061/(ASCE)GT.1943-5606.0000561.
3. S. J. M. van Eekelen, A. Bezuijen, H. J. Lodder, A. F. van Tol, Model experiments on piled embankments. Part I, *Geotext. Geomembr.* **32**, 69–81, (2012). doi: 10.1016/j.geotexmem.2011.11.002.
4. S. J. M. Eekelen, M. H. A. Brugman, Eds., *Design Guideline Basal Reinforced Piled Embankments*, London., 2016. doi: 10.1201/9781315389806.
5. L. Briançon, L. Thorel, B. Simon, Experimental study of pile-supported embankment in the framework of the French research project ASIRI+, in *Proceedings of the 5th International Conference on Transportation Geotechnics (ICTG) 2024*, Volume **8**, C. Rujikiatkamjorn, J. Xue, and B. Indraratna, Eds., Singapore: Springer Nature, 2025, pp. 269–277. doi: 10.1007/978-981-97-8241-3_27.
6. T. Lee, S. H. Lee, I. W. Lee, Y.-H. Jung, Lessons from full-scale experiments on piled embankments with different geosynthetic reinforcements, *KSCE J. Civ. Eng.* **25**, 2, 442–450 (2021), doi: 10.1007/s12205-020-0625-x.
7. F. Lian, Z. Liu, J. Xu, Q. Wang, X. H. Hu, H. Wu, Field Study of Improvement Mechanism of Geogrid-Reinforced and Pile-Supported Embankment, *Appl. Mech. Mater.*, **587–589**,. 928–933 (2014), doi: 10.4028/www.scientific.net/AMM.587-589.928.
8. M. A. Nunez, L. Briançon, D. Dias, Analyses of a pile-supported embankment over soft clay: Full-scale experiment, analytical and numerical approaches, *Eng. Geol.*, **153**, 53–67 (2013). doi: 10.1016/j.enggeo.2012.11.006.
9. J. A. Sloan, Column-supported embankments: Full-scale tests and design recommendations (2011), Accessed: Dec. 18, 2024. [Online]. Available: <http://hdl.handle.net/10919/27931>
10. S. J. M. van Eekelen, A. Bezuijen, H. J. Lodder, A. F. van Tol, Model experiments on piled embankments. Part I, *Geotext. Geomembr.* **32**, 69–81 (2012). doi: 10.1016/j.geotexmem.2011.11.002.
11. S. J. M. Van Eekelen, J. Han, Geosynthetic-reinforced pile-supported embankments: state of the art, *Geosynth. Int.*, **27**, 2, 112–141, (2020). doi: 10.1680/jgein.20.00005.
12. Itasca Consulting Group Inc., *FLAC3D (Fast Lagrangian Analysis of Continua in 3 Dimensions)*, Version 9.0. Minneapolis, MN, USA, 2024. [Online]. Available: <https://www.itascacg.com/software/flac3d>